Naval Research Laboratory
Washington, DC 20375-5320

NRL/MR/6790--08-9096

Incoherent Combining of High-Power Fiber Lasers for Directed-Energy Applications

PHILLIP SPRANGLE
ANTONIO TING
JOSEPH PEÑANO
RICHARD FISCHER

Beam Physics Branch
Plasma Physics Division

BAHMAN HAFIZI

Icarus Research, Inc.
Bethesda, Maryland

January 16, 2008

REPORT DOCUMENTATION PAGE

Form Approved
OMB No. 0704-0188

1. REPORT DATE *(DD-MM-YYYY)*	2. REPORT TYPE	3. DATES COVERED *(From - To)*
16-01-2008	Interim	June 2006 – December 2007

4. TITLE AND SUBTITLE

Incoherent Combining of High-Power Fiber Lasers for Directed-Energy Applications

5a. CONTRACT NUMBER

5b. GRANT NUMBER

5c. PROGRAM ELEMENT NUMBER

6. AUTHOR(S)

Phillip Sprangle, Antonio Ting, Joseph Peñano, Richard Fischer, and Bahman Hafizi*

5d. PROJECT NUMBER
67-9466-08

5e. TASK NUMBER

5f. WORK UNIT NUMBER

7. PERFORMING ORGANIZATION NAME(S) AND ADDRESS(ES)

Naval Research Laboratory
4555 Overlook Avenue, SW
Washington, DC 20375-5320

8. PERFORMING ORGANIZATION REPORT NUMBER

NRL/MR/6790--08-9096

9. SPONSORING / MONITORING AGENCY NAME(S) AND ADDRESS(ES)

Office of Naval Research
One Liberty Center
875 North Randolph St.
Arlington, VA 22203-1995

10. SPONSOR / MONITOR'S ACRONYM(S)

ONR

11. SPONSOR / MONITOR'S REPORT NUMBER(S)

12. DISTRIBUTION / AVAILABILITY STATEMENT

Approved for public release; distribution is unlimited.

13. SUPPLEMENTARY NOTES

*Icarus Research, Inc., P.O. Box 30780, Bethesda, MD 20814-0780

14. ABSTRACT

High-power fiber lasers can be incoherently combined to form the basis of a directed high-energy laser system. This approach has a number of advantages over other beam combining methods and can result in compact, robust, low maintenance and long-lifetime high-energy laser systems. The first field demonstration of incoherent beam combining using kilowatt-class, single-mode fiber lasers over a kilometer propagation range is discussed. The experiment employed four fiber lasers and a beam director consisting of individually controlled steering mirrors. Propagation efficiencies greater than 90% at power levels of 3 kilowatts were demonstrated at a range greater than 1 kilometer.

15. SUBJECT TERMS

High-power fiber lasers
Incoherent beam combining

16. SECURITY CLASSIFICATION OF:			17. LIMITATION OF ABSTRACT	18. NUMBER OF PAGES	19a. NAME OF RESPONSIBLE PERSON
a. REPORT	b. ABSTRACT	c. THIS PAGE			Phillip Sprangle
Unclassified	Unclassified	Unclassified	UL	14	19b. TELEPHONE NUMBER *(include area code)* (202) 767-3493

Standard Form 298 (Rev. 8-98)
Prescribed by ANSI Std. Z39.18

CONTENTS

Abstract 1

I. Introduction 2

II. Atmospheric Propagation of Incoherently Combined Beams 3

III. Single and Multi-Mode Laser Propagation in Turbulence 4

a) Spot Size, Maximum Intensity and Propagation Efficiency 5

b) Comparison of Single and Multi-Mode Propagation 6

c) Comparison of Incoherent and Coherent Combining 7

IV. Beam Wander and Tip-Tilt Compensation 8

V. NRL Fiber Laser Experiments 9

a) Comparison of Experiments with HELCAP Simulations 10

b) Comparison of Experiments with Theory 11

VI. Discussions 11

VII. Conclusions 11

Acknowledgements 12

Incoherent Combining of High-Power Fiber Lasers For Directed-Energy Applications

Phillip Sprangle, Antonio Ting, Joseph Peñano, Richard Fischer and Bahman Hafizi[1]

Naval Research Laboratory
Washington, DC 20375
Plasma Physics Division

Abstract

High-power fiber lasers can be incoherently combined to form the basis of a directed high-energy laser system which is highly efficient, compact, robust, low-maintenance and has a long operating lifetime. This approach has a number of advantages over other beam combining methods. We present results of the first field demonstration of incoherent beam combining using kilowatt-class, single-mode fiber lasers. The experiment combined four fiber lasers using a beam director consisting of individually controlled steering mirrors. Propagation efficiencies of ~ 90 %, at a range of 1.2 km, with transmitted CW power levels of 3 kilowatts were demonstrated in moderate atmospheric turbulence. We analyze the propagation of combined single-mode and multi-mode beams in atmospheric turbulence and find good agreement between theory, simulations and experiments.

[1] Icarus Research, Inc., PO Box 30780, Bethesda, MD 20824-0780

Manuscript approved December 21, 2007

NRL/MR/6790-08-9096

I. Introduction

Technical advances have made fiber lasers a leading candidate for directed-energy (DE) applications. To achieve the necessary power levels, a large number of fiber lasers must be combined. Fiber lasers can be combined coherently, spectrally or incoherently. Incoherent combining of fiber lasers has a number of advantages because it does not require phase locking or polarization locking of the individual lasers, and can be readily scaled up to a compact and reliable DE system. Incoherent combining of laser beams is achieved by overlapping the individual laser beams on a target with a beam director consisting of independently controlled steering mirrors with optional adaptive optics capabilities. Although a number of companies manufacture high-power fiber lasers, IPG Photonics currently holds the record, producing over 3 kW per fiber of single-mode laser radiation [1]. Another company, Nufern expects to have a 1 kW, single-mode fiber laser available early in 2008 [2]. In the present context the term single-mode is synonymous with a diffraction limited, i.e., $M^2 \sim 1$, fundamental Gaussian mode, where M^2 is the conventional "times diffraction limited" parameter. Single-mode beams have the minimum diffractive spreading angle since they do not contain higher order transverse modes. These multi-kW, single-mode fiber lasers are robust, compact, have high wall-plug efficiency, random polarization and large bandwidth ($\sim 0.1\%$). A 1 kW, single-mode IPG fiber laser module, operating at wavelength $\lambda = 1.075\mu m$, excluding power supply, has a dimension of $w \times h \times d \sim 60$ cm $\times 33$ cm $\times 5$ cm, weighs approximately 20 lbs, has a wall-plug efficiency of $\sim 30\%$, and operating lifetime in excess of 10,000 hrs. The total weight of a 2 kW IPG fiber laser, including power supply, is ~ 330 lbs. Because of the high operating efficiency, only a moderate degree of water cooling is required, i.e., ~ 2 gallons/minute/kW. To operate in a single-mode the optical core radius of the fiber must be sufficiently small. For example, the IPG single-mode, 1 kW fiber lasers have an optical core radius of $\sim 15\mu m$. Multi-mode IPG fibers, on the other hand, operating at 10 kW (20 kW) per fiber have optical core radii of ~ 100 μm (~ 200 μm) and $M^2 \sim 13$ ($M^2 \sim 38$). These higher power fiber lasers with larger values of M^2 have a more limited propagation range. In 2008, IPG is expected to have a 5 kW per fiber single-mode laser.

Single-mode fiber lasers are well suited for incoherent combining and high-power, long-range DE applications [3]. Individually-controlled steering mirrors with adaptive optics capabilities form the beam director and direct each beam to the target, as indicated schematically in Fig. 1, which shows an example of a hexagonal array of seven fibers. The individual fiber lasers have an initial spot size large enough so that diffractive spreading is not significant over the propagation range. For example, a single-mode fiber laser with initial spot size $R_o = 4\text{cm}$, has a Rayleigh (diffraction) range of $Z_R = \pi R_o^2/\lambda = 5\text{km}$ and hence, the target range would be less than $\sim 2\, Z_R \sim 10\text{km}$. Usually, however, the spreading of the beam is dominated by atmospheric turbulence and not diffraction.

Incoherent beam combining of fiber lasers is readily scalable to higher total power levels. For N incoherently combined fiber lasers, the total transmitted power is N times the power in the individual fiber and the beam director radius is $R_{BD} \approx \sqrt{N} R_o$. A 500 kW, laser system would consist of 100 fiber lasers (5 kW/fiber), have a beam director

radius of ~ 40 cm and, excluding power supply, the fibers and pump diodes occupy a volume of ~ $8\,m^3$.

In this article we discuss the propagation efficiency of incoherently combined single-mode and multi-mode fiber lasers as a function of propagation range and turbulence level. In a turbulent atmosphere, it is shown that for a given size beam director, the propagation efficiency of incoherently combined single-mode fiber lasers is practically identical to the theoretical upper limit given by that of a single Gaussian beam with a spot size equal to the radius of the beam director. In addition, preliminary results from the Naval Research Laboratory (NRL) field experiments are presented. In these experiments four single-mode fiber lasers, capable of transmitting a total CW power of 6.2 kW, were incoherently combined on a remote target. The total volume occupied by the four fiber lasers, including power supply, diode pump lasers and fibers, is less than 2 m^3. With the lasers at half-power, a total of 3 kW was transmitted over a 1.2 km range to a 10 cm radius target. Propagation efficiencies greater than 90% were demonstrated in a moderately turbulent environment.

II. Atmospheric Propagation of Incoherently Combined Beams

The physical processes affecting the propagation of high-power laser beams in the atmosphere are complicated and interrelated. These processes include diffraction, molecular/aerosol scattering and absorption, turbulence produced by air density fluctuations, thermal blooming, etc. It is beyond the scope of this article to consider these physical processes in detail. However, for the purpose of estimating and comparing the propagation efficiency of combined single-mode and multi-mode fiber lasers we will first consider some of the more important processes in a simplified way, and later discuss the effects of turbulence in greater detail. Here, we define propagation efficiency as the ratio of power on target to total transmitted laser power. We will also discuss the use of tip-tilt compensation to correct for the wander of the beam centroid and quantify its limitations.

The time averaged laser intensity at range L is taken to have a Gaussian profile of the form

$$\langle I(r, z=L) \rangle = I_o \left(R_o / R(L)\right)^2 \exp\left(-2r^2 / R^2(L)\right). \qquad (1)$$

The long time averaged spot size at range L can be written as $R(L) = \left(\Theta^2_{\text{spread}}(L)\, L^2 + R_o^2 \left(1 - L/L_{\text{focal}}\right)^2\right)^{1/2}$ where R_o is the initial spot size, and L_{focal} is the focal length. The minimum laser beam spot size, at a particular range, is obtained by setting $L = L_{\text{focal}}$ and is given by $R = \Theta_{\text{spread}}\, L$ where the spreading angle Θ_{spread} contains contributions from diffraction, Θ_{diff}, beam quality, Θ_{quality}, atmospheric turbulence, Θ_{turb}, mechanical jitter, Θ_{jitter}, and thermal blooming, Θ_{bloom}. For the purpose of discussion, we write the total spreading angle in the form [3]

$$\Theta_{\text{spread}} = \left(\Theta^2_{\text{diff}} + \Theta^2_{\text{quality}} + \Theta^2_{\text{turb}} + \Theta^2_{\text{jitter}} + \Theta^2_{\text{bloom}} \right)^{1/2}. \qquad (2)$$

This expression for the spreading angle is in excellent agreement with the more exact extended Huygens' principle formulation for describing the effects of turbulence.

Thermal blooming, i.e., the self-defocusing of the laser due to absorption and the subsequent heating of the air, can be partially mitigated by propagating in an atmospheric

transmission window where the absorption is low. The fiber laser wavelength, $\lambda = 1.075\,\mu\mathrm{m}$, is near a water vapor transmission window, $\lambda = 1.045\,\mu\mathrm{m}$. However, in the presence of aerosols the actual transmission window is broadened [4] and includes the fiber laser wavelength. For total laser power levels less than ~ 100 kW, and depending on the transverse air flow and atmospheric absorption, thermal blooming effects can usually be neglected [4]. Thermal blooming near the beam director can be eliminated by introducing a transverse air flow. For the purpose of discussion we will also neglect the small mechanical jitter contribution.

The diffractive spreading angle due to multi-mode effects, i.e., beam quality, is $\Theta_{\text{quality}} = (\mathrm{M}^2 - 1)\Theta_{\text{diff}}$, where the diffraction angle of a single-mode beam is $\Theta_{\text{diff}} = \lambda/(\pi R_o)$. For single-mode fibers propagating over long distances, the turbulence contribution usually dominates diffractive and beam quality spreading, i.e., $\Theta_{\text{turb}} >> \Theta_{\text{diff}} >> \Theta_{\text{quality}}$, where $\Theta_{\text{turb}} = 1.6\lambda/\pi r_o$ is the long time averaged spreading angle for a focused beam in strong turbulence, $r_o = 0.184(\lambda^2/C_n^2 L)^{3/5}$ is the Fried parameter (i.e., plane wave transverse coherence radius), and C_n^2 is the index structure constant which is a measure of the turbulence level [5-7]. On the other hand, for multi-mode fibers ($\mathrm{M}^2 >> 1$), the beam quality contribution to the spreading angle can be large, i.e., $\Theta_{\text{quality}} > \Theta_{\text{turb}} >> \Theta_{\text{diff}}$. These differences between single-mode and multi-mode fibers have important consequences for the propagation efficiency and the use of adaptive optics to reduce the effects of turbulence. For single-mode fibers, the use of adaptive optics can substantially improve the propagation efficiency. However, for multi-mode fibers, adaptive optics will have little effect on the propagation efficiency because the dominant contribution to the spreading angle is usually due to beam quality, not turbulence.

III. Single and Multi-Mode Laser Propagation in Turbulence

Propagation through atmospheric turbulence results in spreading of the laser spot size and wandering of the beam centroid. Here, we derive a general expression for the long time-averaged spot size for single and multi-mode beams propagating through turbulence, and compare their propagation efficiencies.

The propagation of laser beams in the atmosphere can be divided into the weak or strong turbulence regimes. The laser beam propagation characteristics, such as the spot size and centroid wander, depend on the turbulence regime which is characterized by the Rytov parameter,

$$\sigma_R^2 = 1.23 C_n^2 k^{7/6} L^{11/6} = 0.63\left(\lambda L / r_o^2\right)^{5/6}, \qquad (3)$$

where r_o is the Fried parameter. The Fried parameter is shown in Fig. 2 as a function of range for various values of C_n^2. The weak fluctuation regime corresponds to the conditions $\sigma_R^2 < 1$ and $\sigma_R^2 (L/Z_{RO})^{5/6} < 1$, where $Z_{RO} = \pi R_o^2/\lambda$ is the Rayleigh length in vacuum associated with the initial spot size R_o. The strong fluctuation regime is characterized by $\sigma_R^2 > 1$ or $\sigma_R^2 (L/Z_{RO})^{5/6} > 1$. As an example, consider the case of the NRL field experiments discussed later where the laser wavelength is $\lambda = 1\,\mu m$, the range

is $L = 1.2\,\mathrm{km}$, $C_n^2 = 5\times10^{-14}\,\mathrm{m}^{-2/3}$ and the Fried parameter is $r_o = 1.6\,\mathrm{cm}$. The Rytov parameter for this case is $\sigma_R^2 = 0.63\left(\lambda L / r_o^2\right)^{5/6} = 2.3$, which characterizes a moderate turbulence regime.

a) Spot Size, Maximum Intensity and Propagation Efficiency

The propagation characteristics of single and multi-mode laser beams can be heuristically derived from the well-known formulation for single-mode beams. For a single-mode Gaussian laser beam the long time-averaged intensity, as a function of radial position r and propagation distance z, can be written as [7]

$$\left\langle I(r,z)\right\rangle = 2\pi I_o\left(\frac{k}{2\pi z}\right)^2\left(\frac{\pi R_o^2}{2}\right)\int_0^\infty d\eta\,\eta\exp\left(-\frac{k^2 R_V^2(z)}{8z^2}\eta^2\right)\times \\ J_o\left(\frac{k\eta r}{z}\right)\exp\left\{-\frac{zC_n^2}{\lambda^2}\left(\varepsilon_1\eta^{5/3} - \varepsilon_2\eta^2/L_o^{1/3}\right)\right\}, \tag{4}$$

where $\varepsilon_1 = 21.9$ and $\varepsilon_2 = 15.6$, L_0 is the outer-scale length associated with the turbulence, and $R_V(z)$ is the laser spot size for vacuum propagation. The laser intensity in Eq. (4) is for an ideal Gaussian beam which formally has a beam quality $M^2 = 1$. Multi-mode lasers, however, are characterized by the beam quality factor $M^2 >> 1$. To estimate the average intensity for multi-mode laser beams in turbulence we set

$$R_V^2(L) = M^4\,\Theta_{\mathrm{diff}}^2\,L^2 + R_o^2\left(1 - L/L_{\mathrm{focal}}\right)^2, \tag{5}$$

which is the spot size (squared) of a multi-mode beam propagating in vacuum. In vacuum, the minimum spot size at a given target range, L, is obtained by setting $L = L_{\mathrm{focal}}$, while, for a given focal length, the spot size is minimum at $L = L_{\mathrm{focal}}/(1+M^4\,\Theta_{\mathrm{diff}}^2\,L_{\mathrm{focal}}^2/R_o^2)$.

Equating Eqs. (1) and (4) for $r=0$, an expression for the long time averaged spot size can be obtained. The spot size (squared) for single and multi-mode lasers propagating in a turbulent atmosphere without adaptive optics is found to be

$$R^2(z) = R_V^2(z)\,G(z), \tag{6}$$

where $R(z) = \sqrt{R_{ST}^2(z) + R_{\mathrm{wander}}^2(z)}$ is the long time averaged spot size which includes contributions from the short time spot size R_{ST} and the centroid wander R_{wander} (see Fig. 3). The function $G(z)$ characterizes the increase in spot size due to turbulence and is given by

$$G(z) = \left(\int_0^\infty d\xi\exp(-a(z)\xi - b(z)\xi^{5/6})\right)^{-1}, \tag{7}$$

where $a(z) = 1 - 0.19\,\beta^2(z)(r_o(z)/L_o)^{1/3}$, $b(z) = 0.35\,\beta^{5/3}(z)$, and $\beta(z) = \lambda z/(r_o(z)\,R_V(z))$. The outer-scale is typically large, $L_o \sim 100\,\mathrm{m}$, and the function $a(z) \approx 1$. The function $G(z)$ is well approximated by $G(z) = 1 + 2.6\,\beta^2(z)$ over the full range of the parameter β.

Figure 4 plots the spot size, $R(z)$, as a function of propagation distance, z, for a focused beam with $L_{\text{focal}} = 5$ km. For a target at $z = L_{\text{focal}}$, this results in the minimum spot size *on target*. Note that, even in vacuum, L_{focal} does not denote the position of the beam "waist", which occurs before the target. Various curves represent $C_n^2 = 0$ (green), 10^{-15} $\text{m}^{-2/3}$ (blue), and 10^{-14} $\text{m}^{-2/3}$ (red). Panel (a) is plotted for a single-mode beam ($M^2 = 1$), panel (b) is plotted for a multi-mode beam ($M^2 = 7$). Figure 4 shows that the spot size on target is a strong function of the turbulence level for the single-mode case, while for the multi-mode case, the spot size on target is not a strong function of turbulence since it is determined mainly by diffractive effects.

The long time averaged spot size (squared) of a focused beam ($L = L_{focal}$) on target is

$$R^2(L) = \left(\frac{\lambda L}{\pi R_o}\right)^2 \begin{cases} M^4 + 2.6(R_o/r_o)^2, & \text{strong turbulence} \\ M^4 + 2.16(R_o/r_o)^{5/3}, & \text{weak turbulence} \end{cases}. \qquad (8)$$

Figure 5 plots the spot size on target, $R(L)$, versus range for a focused beam with $L = L_{\text{focal}}$ for various initial spot sizes, R_o. Curves denote propagation in vacuum (dashed curves) and in turbulence (solid curves) with $C_n^2 = 10^{-14}\,\text{m}^{-2/3}$. Comparing the dashed curves with the solid curves indicates that for the single-mode case (Fig. 5(a)), turbulence has a more significant effect on the spot size than does diffraction. In the multi-mode case (Fig. 5(b)), the propagation diffractive spreading is more important than turbulence spreading.

In the strong turbulence regime, average intensity on axis is

$$\langle I(r=0,L)\rangle = \left(\frac{2.4P_o}{1 + 3.8(M^2 r_o/R_o)^2}\right)\left(\frac{r_o}{\lambda L}\right)^2, \qquad (9)$$

where $P_o = I_o \pi R_o^2/2$ is the transmitted power. If the initial laser beam spot size is large ($R_o >> M^2 r_o$), the spot size and maximum intensity on axis at range L become $R(L) = 1.6(\lambda L/\pi r_o)$, and $\langle I(r=0,L)\rangle_{\max} = 2.4P_o(r_o/\lambda L)^2$, respectively. As an example, assuming $P_o = 1\text{kW}$, $L = 1\text{km}$, $r_o = 4.6\text{cm}$ ($C_n^2 = 10^{-14}\,\text{m}^{-2/3}$) and $\lambda = 1\mu\text{m}$, the maximum intensity is $\langle I(r=0,z)\rangle_{\max} \approx 500\,\text{W/cm}^2$.

The propagation efficiency, i.e., ratio of power on target to transmitted power, is defined by

$$\eta_{\text{prop}} = 2\pi P_o^{-1} \int_0^{R_T} dr\, r \langle I(r,L)\rangle = \exp(-\gamma L)\left(1 - \exp(-2R_T^2/R^2)\right), \qquad (10)$$

where R_T is the target radius and γ is the extinction coefficient, i.e., scattering and absorption.

b) Comparison of Single and Multi-Mode Propagation

It is useful to compare the propagation efficiency of incoherently combined single-mode and multi-mode fiber lasers having the same size beam director and the

same total power. Table I lists the parameters of four systems that are designed to deliver a total power of 100 kW. The systems are based on currently available fiber lasers. For example, for the 3 kW/per fiber, $M^2 = 1$ case, 33 fibers are required. The corresponding M^2 values reflect the fact that the M^2 increases as the modal content of the fibers increase. Table I also gives the radius of the collimating lens for the individual fiber lasers. In all cases the radius of the beam director is 50 cm. The target is assumed to be a circular disc with a surface area of 100 cm^2. Figure 6 plots the propagation efficiency for M^2 = 1, 7 and 38, in vacuum (Fig. 6(a)), and in a turbulent environment with $C_n^2 = 10^{-14}\ m^{-2/3}$ (Figs. 6(b) and (c)). The propagation efficiency is calculated using Eqs. (6) and (10). For propagation through turbulence, the figure shows the efficiency without (b) and with (c) adaptive optics. Adaptive optics was incorporated into the results shown in Fig. 6(c) by increasing the Fried parameter by a factor of four. The dashed curves denote the case of a single Gaussian beam with initial spot size equal to the radius of the beam director, i.e., the theoretical upper limit for both coherent and incoherent combining. For ranges < 10 km in vacuum (Fig. 6(a)), and for conditions in which turbulence dominates (Fig. 6(b)), the single-mode incoherently combined example (red curve) has a propagation efficiency which is virtually identical to that of the ideal Gaussian beam (dashed curve), while the propagation efficiency of the various multi-mode fibers is far less. Figure 6 also shows that the use of adaptive optics can greatly improve the propagation efficiency of combined single-mode fibers but has little effect on the efficiency of combined multi-mode fiber lasers.

c) Comparison of Incoherent and Coherent Combining

It is commonly stated that for incoherent beam combining, the effective beam quality associated with the combined single-mode Gaussian beams is $M_{\text{eff}}^2 = \sqrt{N}$, where N is the number of lasers. This would imply that, in the far-field regime (propagation range greater than the Rayleigh range of an individual beam), the effective vacuum spreading angle of incoherently combined beams is $\sqrt{N}$ times greater than for a coherently combined laser array with the same size beam director. However, this fact is not relevant for two reasons. First, since the ranges of interest (< 10 km) are comparable to the Rayleigh length associated with an individual beam, diffractive spreading is not a major limitation. For example, in Figure 6(a), the propagation efficiency in vacuum for both the ideal, single Gaussian beam (dashed) and single-mode incoherently combined beams (red) is nearly 100% for ranges less than ~8 km. Second, and perhaps more important, beam spreading due to atmospheric turbulence typically dominates diffractive spreading, i.e., r_o is usually less than R_o. As shown in Fig. 6(b), in the presence of turbulence, the curve for incoherently combined single-mode lasers with $N = 33$ is always near the theoretical $(M^2 = 1)$ limit. For the same size beam director, it can be shown that the spreading angles for single-mode incoherently combined beams and coherently combined beams are essentially identical when $r_o << R_o = R_{BD}/\sqrt{N}$. This condition is satisfied for typical atmospheric turbulence levels and propagation ranges. Hence, there is no inherent advantage to coherently combining beams for directed energy

applications when turbulence dominates or for propagation ranges in the near and intermediate field regimes, which is typically the case.

IV. Beam Wander and Tip-Tilt Compensation

Introducing tip-tilt correction into the individual steering mirrors can reduce the long time spot size by reducing beam wander. The distribution of scale sizes for turbulent eddies in the atmosphere is bounded by the inner and outer scale lengths, ℓ_o and L_o, respectively. The outer scale length ranges from 1 m to 100 m while the inner scale length is ~ 1 mm. The turbulent eddies that are large compared to the laser beam diameter cause the beam centroid to be deflected and to wander in time due to transverse air flow. The beam centroid wanders with a characteristic time equal to the transit time, $\sim 2R/V$ where V is the transverse air flow velocity. The small scale length eddies cause the beam's short term spot size to increase about the centroid. The observed long time, averaged spot size is a combination of these two effects.

In the weak turbulence regime the beam centroid wander represents a significant contribution to the long time beam radius. As the turbulence level increases due to increasing values of C_n^2 and/or increasing propagation ranges, the beam wander contribution becomes relatively less important to the long time beam spreading. When the turbulence is sufficiently strong that beam spreading dominates wander, tip-tilt adaptive optics will not be effective. The condition for this to occur is given below.

The ratio of the intensity on target with perfect tip-tilt correction to the intensity without tip-tilt correction, i.e., the intensity gain, is

$$\beta \equiv \frac{\langle I(0,L)\rangle_{\text{tip-tilt}}}{\langle I(0,L)\rangle_{\text{no tip-tilt}}} = \frac{1}{1 - R_{\text{wander}}^2 / R^2}, \tag{11}$$

The general expression for the centroid wander (squared), in both the weak and strong turbulence regimes, is given by [5],

$$R_{\text{wander}}^2(L) = 7.25 \frac{C_n^2 L^3}{R_o^{1/3}} F = 0.43 \frac{(\lambda L)^2}{(R_o r_o^5)^{1/3}} F, \tag{12}$$

where $F = \int_0^1 d\xi\, \xi^2 \left[g^{-1/6}(\xi) - \varepsilon_o^{1/3} (1 + \varepsilon_o^2\, g(\xi))^{-1/6} \right]$,

$$g(\xi) = \begin{cases} \xi^2 + 1.63\, \sigma_R^{12/5} (1 - \xi)^{16/5}\, L/Z_{RO}, & \text{(focused)} \\ 1 + 1.63\, \sigma_R^{12/5} (1 - \xi)^{16/5}\, L/Z_{RO}, & \text{(collimated)} \end{cases}$$

for focused and collimated beams, $\varepsilon_o = \kappa_o R_o$, and $1/L_o < \kappa_o < 8\pi/L_o$. For a focused beam, the wander in the weak and strong turbulence regimes is given by

$$R_{\text{wander}}^2 = 0.16 \frac{\lambda^2 L^2}{\left(R_o r_o^5\right)^{1/3}} \begin{cases} 1, & \text{weak turbulence } (\sigma_R^2 << 1) \\ 3.9 \left(R_o r_o / \lambda L\right)^{1/3}, & \text{strong turbulence } (\sigma_R^2 >> 1). \end{cases} \tag{13}$$

In deriving Eq. (13), it was assumed that the outer scale length $L_o \to \infty$. For a focused beam the ratio of Eq.(13) to the long time spot size squared is

$$\frac{R^2_{\text{wander}}(L)}{R^2(L)} = \begin{cases} \dfrac{0.73}{1+0.46(r_o/R_o)^{5/3}} \approx 0.73, & \text{weak turbulence} \\ \dfrac{2.78(r_o^2/\lambda L)^{1/3}}{1+r_o^2/(2.7R_o^2)} \approx 2.78(r_o^2/\lambda L)^{1/3}, & \text{strong turbulence} \end{cases} . \quad (14)$$

Adaptive tip-tilt compensation will not be very effective when the ratio in Eq. (14) is much less than unity. Figure 7 plots the intensity gain due to tip-tilt correction (Eq. (11)) as a function of C_n^2 for different target ranges. All curves represent cases of strong turbulence in which the Rytov parameter is comparable or much greater than unity. For $C_n^2 < 10^{-14}$ m$^{-2/3}$, tip-tilt correction can enhance the intensity on target by ~ 50%. The improvement due to tip-tilt correction decreases with turbulence strength for $C_n^2 > 10^{-14}$ m$^{-2/3}$.

For propagation distances $L >> (2\pi/\lambda)\min(r_o^2, 4R^2) \sim 1$km, it is expected that the beam will break up into multiple beamlets making tip-tilt compensation impossible. In this case the beam centroid wander has little relevance, but the long time averaged spot size given by Eq. (6) is still applicable.

Analysis and simulations indicate that if individual beams are separated by less than r_o at the source, the wander of the centroids on the target will be correlated. In this case, it may be possible for beams to share a common tip-tilt correcting aperture, thus reducing the size and complexity of the system.

V. NRL Fiber Laser Experiments

The NRL incoherent combining field experiments use four IPG single-mode fiber lasers having a total output power of 6.2 kW (1 kW, 1.6 kW, 1.6 kW and 2 kW). Initial experiments have taken place at the Naval Surface Warfare Center (NSWC) in Dahlgren, VA over a propagation range of 1.2 km. These experiments have demonstrated ~ 90% propagation efficiency for ~ 3 kW of transmitted laser power. In these initial experiments the fiber lasers were operated at nearly half power because of thermal blooming in the beam director and in the atmosphere just beyond the laser source. These issues can be readily corrected in the next series of experiments by using better, low-absorption optics and inducing air flow near the laser output.

The beam director consists of four fiber output couplers and individually controlled steering mirrors which direct the four single-mode fiber laser beams onto a target. Each beam has a spot size of ~ 2.5 cm as it exits the beam director and the target is a 10 cm radius, water-cooled power meter.

Figure 8 shows a schematic of the fiber laser output coupler and the beam expander (concave-convex lens combination) which is used to adjust the focal length. In these initial experiments thermal effects in the beam director limited the total transmitted power. Thermal effects caused an axial shift of the focus with time as the total laser power was increased to ~ 3 kW. The change in the focal length was compensated for by changing the separation between the lenses in the beam expander. Figure 9 shows the beam director, output couplers, and steering mirrors used in the experiments.

The power on target as a function of time is shown in Fig. 10. After the output coupler reaches thermal equilibrium (> 200 sec) the measured power was 2.8 kW, corresponding to a propagation efficiency of ~ 90%. Air turbulence causes the beams on the target to wander and change shape with time. At times, the four beams completely overlap forming a single spot. At other times four individual beams can be observed separated by a few centimeters. The characteristic time associated with beam wander is $R/V \sim 20\,\text{msec}$. Since the mechanical jitter angle was measured to be less than ~ 2 μ rad, the beam centroid wander is caused mostly by atmospheric turbulence.

Figure 11 displays two frames from a CCD camera, the first at ~ 180 sec and the second at ~ 300 sec, showing 2.8 kW of combined laser power on the power meter. The two frames were chosen to show cases where the four centroids are fully overlapped and where they have maximum displacement from each other. The typical errors associated with the transmitted and target power meters are $\pm 5\%$.

Precise measurements of beam wander and spreading at the target are difficult and were not available for these preliminary experiments because of pixel saturation in the camera and a limited number of frame samples. However, one can estimate the beam wander and short term spot size from the CCD images. For example, the lower panel of Fig. 11 shows that the average centroid wander is ~ 4 cm and the individual bright spots have radii of ~ 2.5 cm, which is taken to be the short time spot size, R_{ST}. The long time averaged spot size is then estimated to be $R \sim \sqrt{(4\text{ cm})^2 + (2.5\text{ cm})^2} \sim 4.7\text{ cm}$.

a) Comparison of Experiments with HELCAP Simulations

The simulation code used to model the experiments is the Navy's **H**igh-**E**nergy **L**aser **C**ode for **A**tmospheric **P**ropagation (HELCAP) [3,4,8] which is fully 3-dimensional, time-dependent and includes molecular/aerosol scattering/absorption, turbulence and thermal blooming effects. To compare the experimental observations with HELCAP simulations, C_n^2 was measured using a scintillometer and used as an input to the code. The average value of C_n^2 during the experiments was measured to be $\approx 5\times10^{-14}\ \text{m}^{-2/3}$ and the average transverse wind velocity was estimated to be ~ 2.5 m/sec. The simulations assume an aerosol scattering coefficient of 0.05 km^{-1} [3] and 1 μrad of mechanical jitter.

Figure 12 shows the results of HELCAP simulations for incoherent combining of the four laser beams with a total power of 3 kW, over a range of 1.2 km. Panel (a) shows the intensity contours of the four beams at the fiber laser output coupler. The focal length of each beam is adjusted to yield the minimum spot size on target. Panel (b) shows time-averaged (over a few seconds) intensity contours of the combined laser beam on the target plane. The combined beam at 1.2 km has a spot size of ~ 4.7 cm. The intensity profile as a function of time shows the wandering of four beams, each with an rms displacement of $R_{\text{wander}} = 2.5\,\text{cm}$. The rms short time spot size of individual beams were measured to be $R_{ST} = 3.1$ cm in the simulations. These simulation results are in good agreement with those observed in the experiments as shown in Fig. 11.

Figure 13 plots the propagation efficiency contained within a given target radius as a function of the radius. Approximately 94% of the transmitted power is contained

within a radius of ~ 10 cm on the target plane. In the absence of aerosol scattering, the propagation efficiency for a 10 cm target is ~ 100%.

b) Comparison of Experiments with Theory

Since the initial beam separation is much greater than r_o the individual beams are uncorrelated and their centroids are randomly displaced with respect to each other, as observed. For the NRL experiments ($\lambda = 1\mu m$, $L = 1.2\text{km}$, $C_n^2 = 5\times10^{-14}\,\text{m}^{-2/3}$ and $r_o = 1.6\text{cm}$), the Rytov parameter is $\sigma_R^2 = 0.63\left(\lambda L / r_o^2\right)^{5/6} = 2.3$ which characterizes a moderate turbulence regime. Since the propagation is in the moderately turbulent regime we use the general expression for beam wander in Eq. (12) and find $R_{\text{wander}} = 2.8\text{cm}$. The long time spot size is found from Eq. (8), with $R_o = 2.5\text{cm}$ and $M^2 = 1$, to be $R = 4.2\text{cm}$ and the short time spot size is $R_{ST} = \sqrt{R^2 - R_{\text{wander}}^2} = 3.2\text{cm}$. These theoretical values are in good agreement with both the experimental and numerical modeling (HELCAP) results.

VI. Discussions

Early in 2008, the NRL fiber lasers will be moved to the Starfire Optical Range in Albuquerque, NM and propagation experiments over a 3.2 km range will take place at full power. The objectives of these experiments are to demonstrate the incoherent beam combining concept at longer range, quantify thermal blooming effects, more precisely characterize the beam wander and spreading, and validate the propagation models. Planned experiments will incorporate target-in-the-loop tip-tilt adjustments into one of the fiber laser beams to correct for wandering of the beam centroid. Controlled thermal blooming experiments can also be carried out using a stagnation tube to eliminate the cooling effects of transverse air flow. This arrangement permits thermal blooming effects to be observed at relatively low power levels. Analysis indicates that a 5-meter-long stagnation tube at the source will result in observable laser beam spreading on the target at a range of 1.2 km. The temporal change in the laser spot size and intensity and measurements of the air properties inside the stagnation tube will provide the necessary data to study atmospheric thermal blooming under realistic conditions.

In addition to the NRL program, other fiber laser based DE efforts are underway. A NAVSEA lethality/propagation program being carried out at NSWC utilizes six multi-mode fiber lasers, each having a CW power of 5 kW and optical quality of $M^2 \sim 6$. A joint Pennsylvania State University/Crane lethality and propagation program is also underway using two, 10 kW ($M^2 \sim 13$) and 5kW ($M^2 \sim 6$), multi-mode fiber lasers.

VII. Conclusions

Incoherent combining of high-power fiber lasers can result in highly efficient, compact, robust, low maintenance, and long-lifetime high-energy laser systems for directed energy applications. In this paper, we have analyzed the propagation of incoherently combined single-mode and multi-mode fiber laser beams through atmospheric turbulence. We have discussed the long time-averaged laser spot size, beam centroid wander, and propagation efficiency of single-mode and multi-mode beams. Under typical atmospheric conditions and propagation ranges, the propagation efficiency

of incoherently combined single-mode fiber lasers is nearly identical to the theoretical upper limit given by that of a single Gaussian beam with a spot size equal to the radius of the beam director. Hence, there is no inherent advantage to coherently combining beams for directed energy applications in the near and intermediate field regimes or when turbulence dominates. In addition, it is commonly believed that the effective beam quality of incoherently combined single-mode beams scales as the square root of the number of fibers and that the beam quality can be poor for a large number of combined fibers. Here again, in realistic atmospheres, when the effects of turbulence are dominant, the effective beam quality of combined single-mode beams plays little role in the propagation.

We have presented results from the first field demonstration experiments of long range incoherent combining. The experiments combined four fiber lasers using a beam director consisting of individually controlled steering mirrors. Propagation efficiencies of ~ 90%, at a range of 1.2 km, with transmitted CW power levels of 3 kilowatts were demonstrated in moderate turbulence. The experimental results agree well with theory and numerical simulations using the HELCAP code.

The initial NRL propagation experiments have provided important information concerning the issues associated with incoherently combining high-power, single-mode fiber lasers. These field experiments lay the ground work for developing a tactical DE laser system in the near-term.

Acknowledgements

This work is sponsored by NRL, ONR and HEL-JTO.

References

[1] "2kW CW Yb-Doped Fiber Laser with Record Diffraction Limited Brightness", V. Gapontsev, CLEO Europe, 2005, CJ1-1-THU, Munich, Germany.

[2] "Kilowatt Level, Monolithic Fiber Amplifiers for Beam Combining Applications at 1 μm", J. Edgecumbe, et.al., Conference Proceeding of Solid State and Diode Laser Technology Review (2007).

[3] "Incoherent combining of high-power fiber lasers for long-range directed energy applications", P. Sprangle, J. Peñano, B. Hafizi, and A. Ting, Journal of Directed Energy, **2**, Spring 2007, pp. 273-284, also NRL Memorandum Report, NRL/MR/6790--06-8963.

[4] "Optimum Wavelength and Power for Efficient Laser Propagation in Various Atmospheric Environments", P. Sprangle, J. Peñano and B. Hafizi, Journal of Directed Energy, **2**, pp. 71-95 (2006).

[5] "Laser Beam Propagation through Random Media," 2nd Ed., L.C. Andrews, R.L. Phillips, SPIE Press, Bellingham, WA (2005).

[6] "Adaptive Optics for Astronomical Telescopes," J.W. Hardy, Oxford University Press, New York, NY (1998).

[7] "Electromagnetic beam propagation in turbulent media," R.L. Fante, IEEE Proc. **63**, 1669 (1975).

[8] "Propagation of High Energy Laser Beams Through Atmospheric Stagnation Zones" J.R. Peñano, P. Sprangle and B. Hafizi, Journal of Directed Energy, **2**, 107 (2006).

Power/fiber [kW]	M^2	N_{fiber}	R_0[cm]
3	1	33	8.7
5	7	20	11.2
20	38	5	22.4
100	1	1	50

Table 1: Various configurations of a 100 kW system using single-mode and multi-mode fiber lasers. Table lists power/fiber, beam quality, the number of fibers required to achieve 100 kW, and the individual beam spot size at the source. The beam director radius is 50 cm. Systems are labeled by color to match propagation efficiency plotted in Fig. 6. The black, dashed curve in Fig. 6 denotes an ideal Gaussian beam having a 50 cm spot-size.

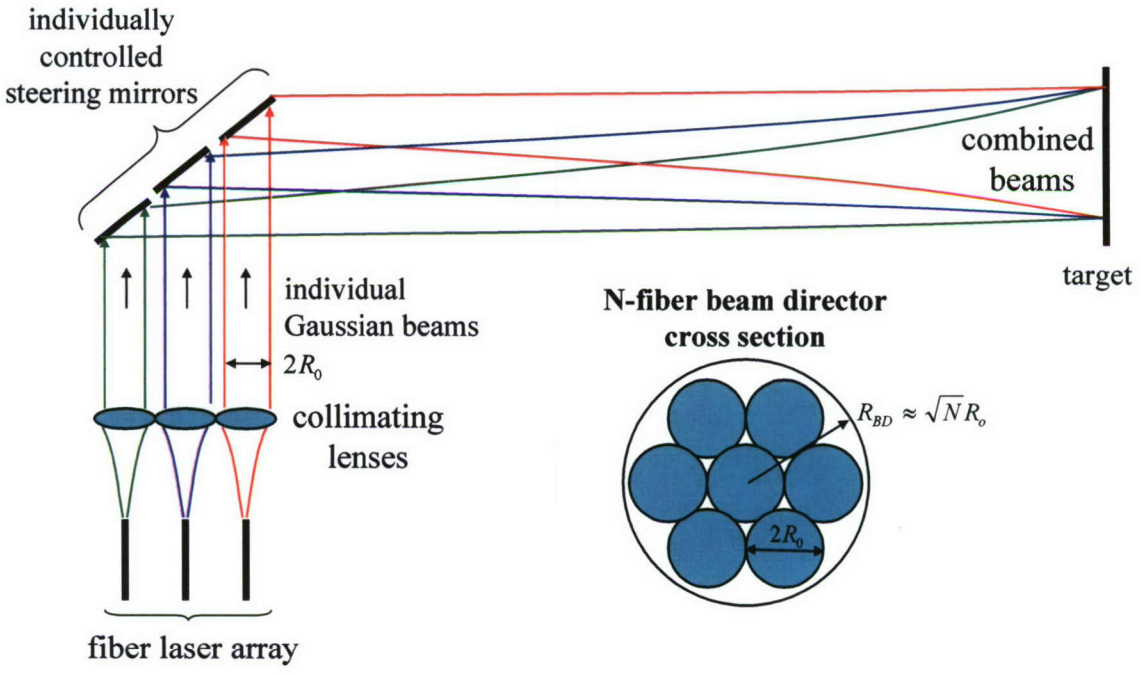

Figure 1: Schematic diagram of incoherently combined fiber lasers individually directed to the target.

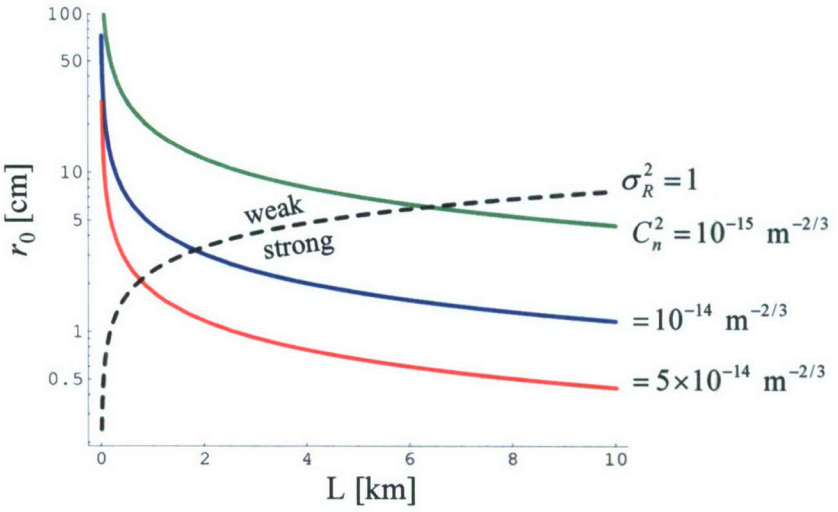

Figure 2: Solid curves: Fried parameter, $r_o(L) = 0.184(\lambda^2 / C_n^2 L)^{3/5}$ vs. range L for $\lambda = 1\,\mu\text{m}$, $C_n^2 = 5\times10^{-14}\,\text{m}^{-2/3}$ (red), $10^{-14}\,\text{m}^{-2/3}$ (blue), and $10^{-15}\,\text{m}^{-2/3}$ (green). Dashed curve: r_o for which the Rytov parameter, $\sigma_R^2 = 0.63\left[\lambda L / r_o^2\right]^{5/6} = 1$, i.e., the boundary between weak and strong turbulence regimes. The expression for the Fried parameter is valid when C_n^2 is uniform and for $\ell_o < r_o < L_o$, where ℓ_o and L_o are the inner and outer scale lengths associated with the turbulence.

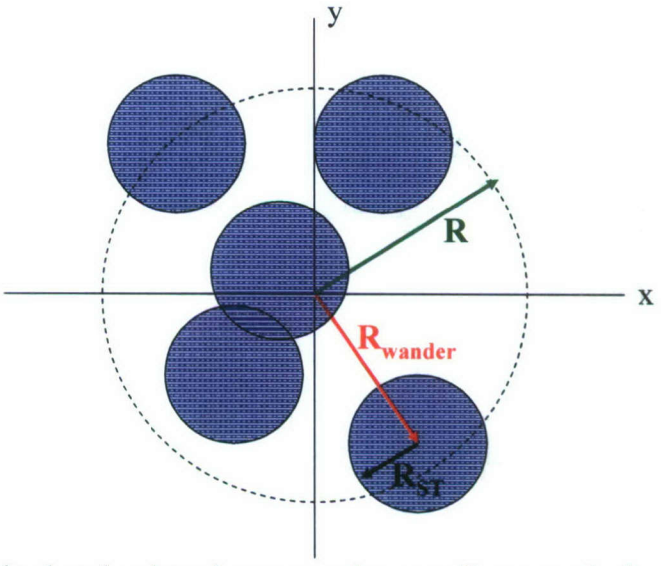

Figure 3: Schematic showing how beam wander contributes to the long time averaged spot size at range L. The blue circles represent the laser spot on the target at various times. R_{wander} denotes the displacement of the beam centroid (wander), R_{ST} denotes the short-time spot size of the beam, and $R = \sqrt{R_{ST}^2 + R_{\text{wander}}^2}$, denotes the long time averaged laser spot size.

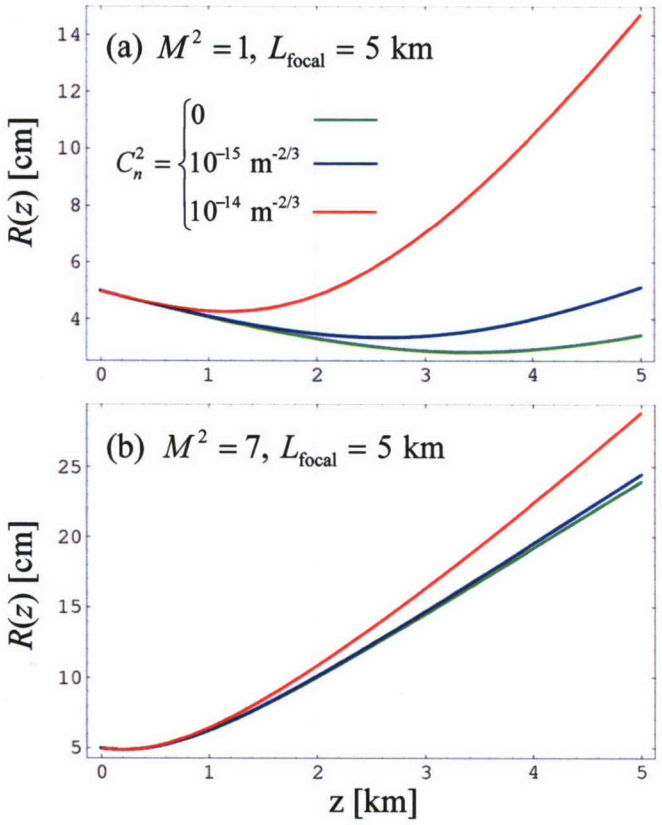

Figure 4: Spot size, $R(z)$ versus propagation distance, z, for a focused beam with an initial spot size $R_0 = 5$ cm and $L_{\text{focal}} = 5$ km. For a target at $z = 5$ km, this results in the minimum spot size on target. Various curves represent $C_n^2 = 0$ (green), 10^{-15} m$^{-2/3}$ (blue), and 10^{-14} m$^{-2/3}$ (red). Panel (a) is plotted for a single-mode beam $(M^2 = 1)$, panel (b) is plotted for a multi-mode beam $(M^2 = 7)$.

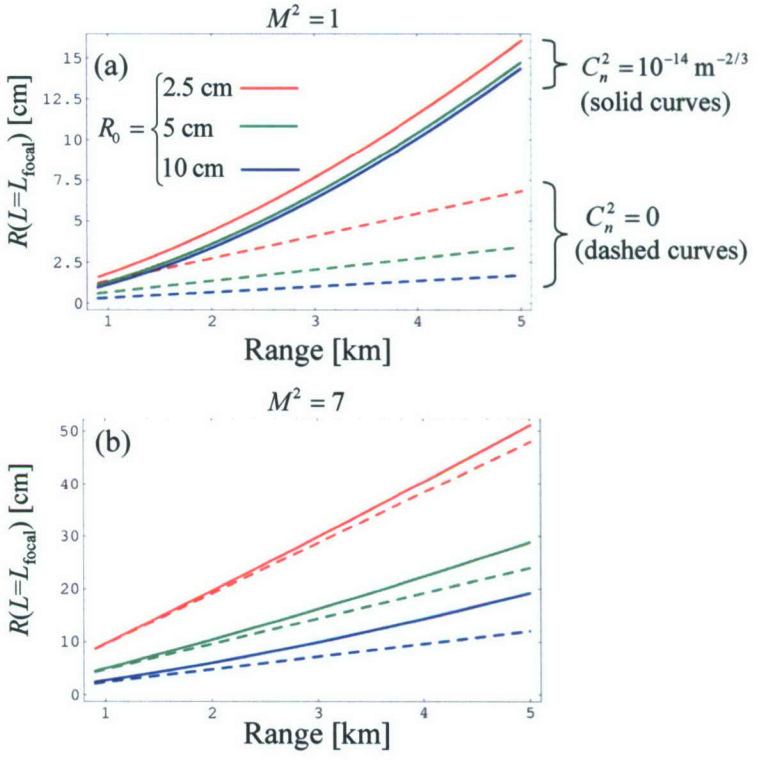

Figure 5: Minimum spot size on target, $R(L)$, versus range for a focused beam ($L = L_{\mathrm{focal}}$) with various initial spot sizes, R_o. Panel (a) shows the single-mode ($M^2 = 1$) case, panel (b) shows a multi-mode ($M^2 = 7$) case. Curves denote propagation in vacuum (dashed curves) and in turbulence (solid curves) with $C_n^2 = 10^{-14}\ \mathrm{m}^{-2/3}$. Spot size is obtained from Eq. (6).

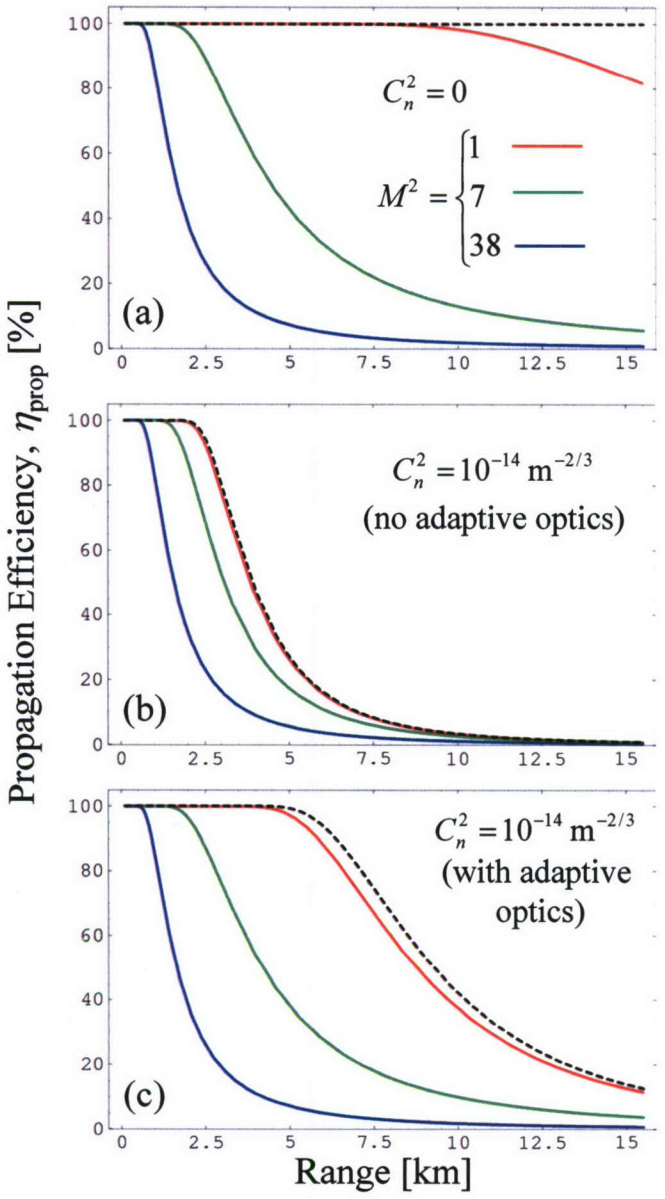

Figure 6: Propagation efficiency versus range for incoherently combined fiber laser beams with beam quality parameters M^2 = 1, 7 and 38: (a) in vacuum, (b) in a turbulent atmosphere with $C_n^2 = 10^{-14}\,\mathrm{m}^{-2/3}$ (no adaptive optics), and (c) in a turbulent atmosphere with adaptive optics. The target is a circular disc with a surface area of 100 cm^2 at a range L. Beams are focused onto the target, i.e., $L = L_{\mathrm{focal}}$. Propagation efficiency is calculated using Eqs. (6) and (10). In all cases the total power is 100 kW and the radius of the beam director is $R_{BD} = \sqrt{N} R_0 = 50\,\mathrm{cm}$, where N is the number of beams and R_0 is the spot size of an individual beam. The dashed curve is for a single Gaussian beam with spot size equal to R_{BD}, i.e., the theoretical upper limit for coherent and incoherent combining. Adaptive optics is incorporated into (c) by increasing the Fried parameter by a factor of four.

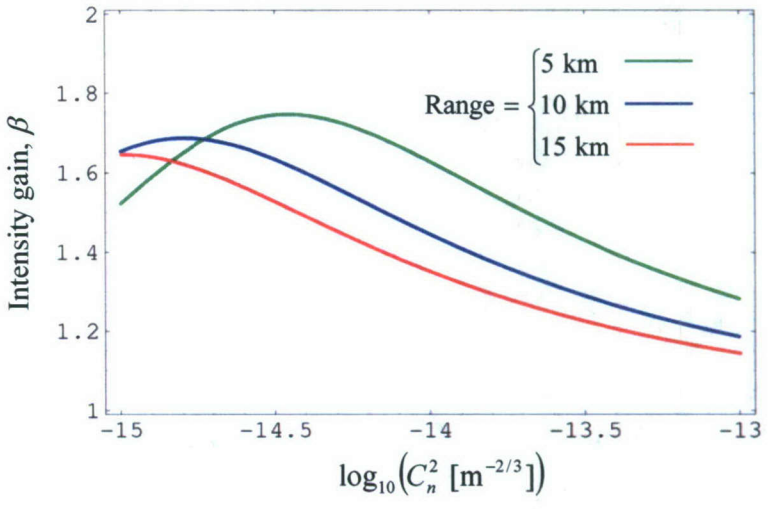

Figure 7: Intensity gain due to tip-tilt correction, $\beta \equiv \langle I(0,L)\rangle_{\text{tip-tilt}} / \langle I(0,L)\rangle_{\text{no tip-tilt}}$, (Eq. 11) versus C_n^2 for various target ranges in moderate to strong turbulence $(\sigma_R^2 \geq 1)$. Beam is assumed to have an initial spot size of $R_0 = 5$ cm and is focused onto the target $(L = L_{\text{focal}})$.

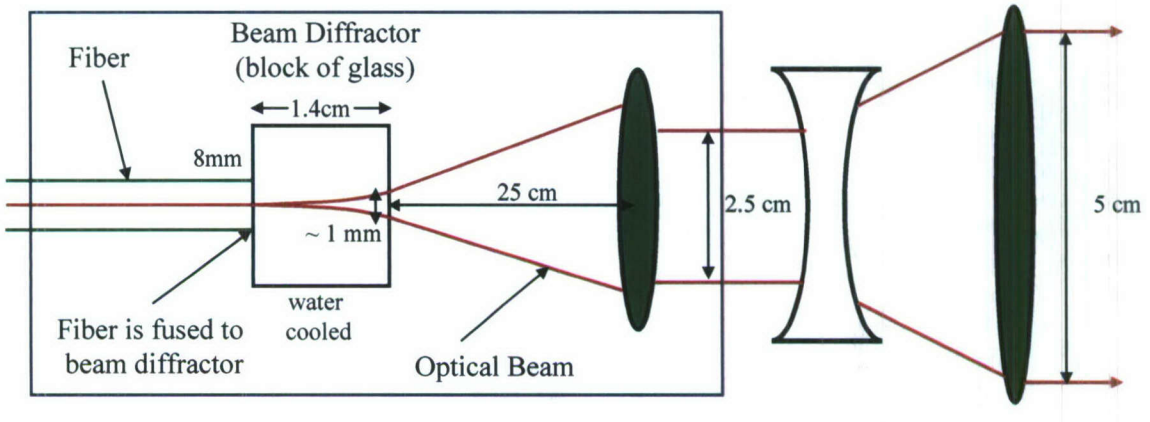

Figure 8: Schematic diagram of fiber output coupler and beam expander.

Figure 9: Beam director used for incoherent combining. Three of four fiber output couplers are shown in the foreground. Four individually controlled steering mirrors are shown in the background.

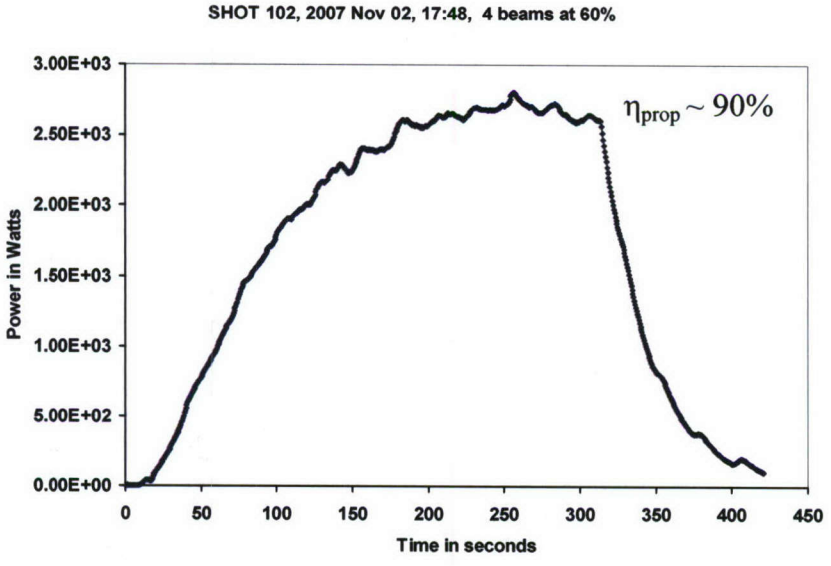

Figure 10: Experimentally measured power at target versus time. Target was a power meter with 45 sec response time and 10 cm radius. Average wind speed was ~ 2.5 m/sec, and measured turbulence strength $C_n^2 = 5 \times 10^{-14}$ m$^{-2/3}$. Transmitted power was 3 kW and the propagation efficiency ~ 90%. The initial power build up is due to the finite power meter response time and temporally changing focal length caused by thermal effects. The fluctuations on the measured power are due to water temperature variations. Thermal equilibrium in the power meter is reached at ~ 200 sec and the laser beams are turned off at ~320 sec.

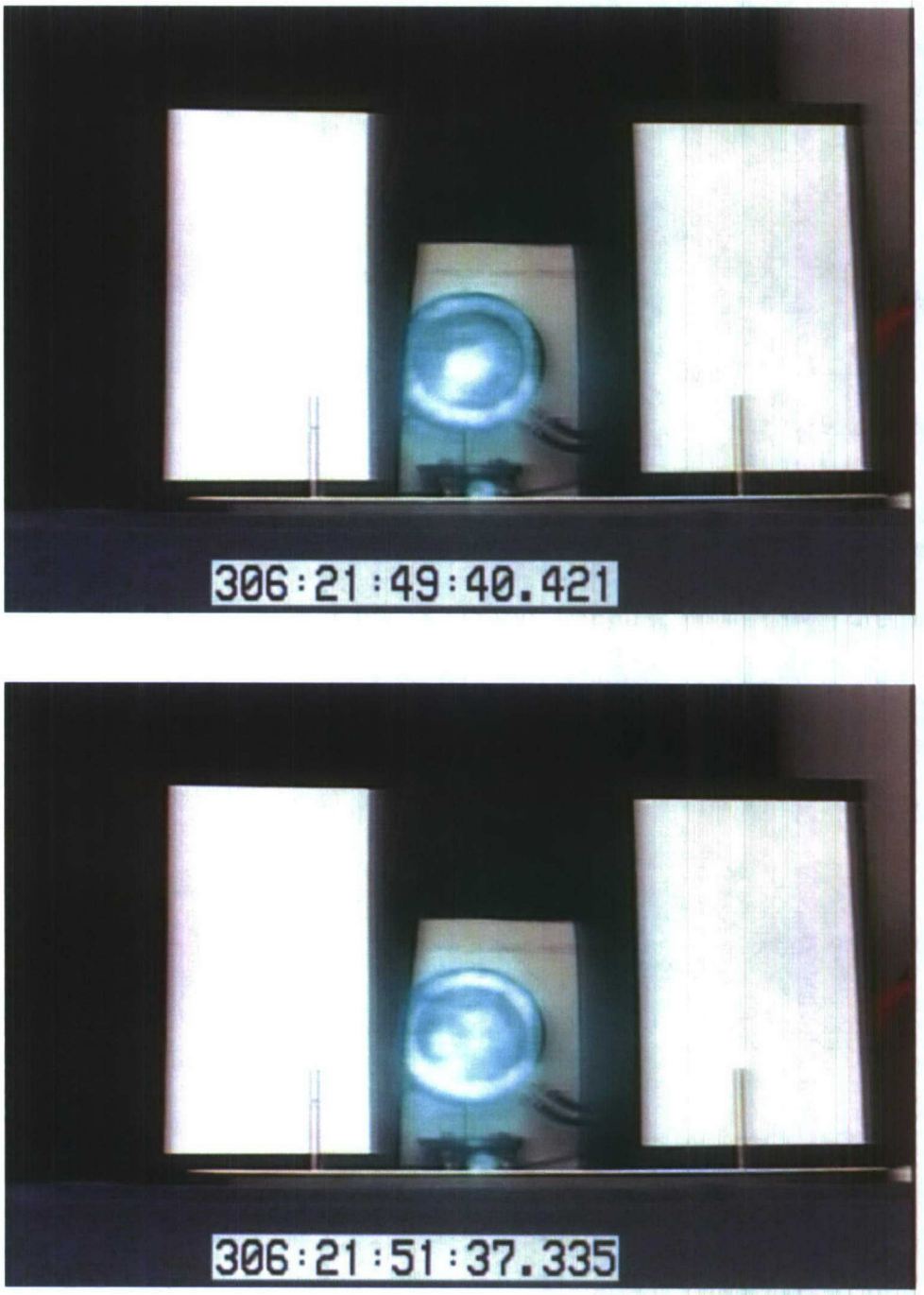

Figure 11: Two CCD camera images of four beams incoherently combined on target (10 cm radius power meter) at a range of 1.2 km. The total transmitted power was 3 kW and the propagation efficiency ~ 90 %. The first panel shows the combined beams at ~ 180 sec and the second image is at ~ 300 sec. The later image shows the four individual beam centroids randomly displaced by ~ 4 cm, which is in good agreement with the beam wander, R_{wander}, obtained from theory and simulations.

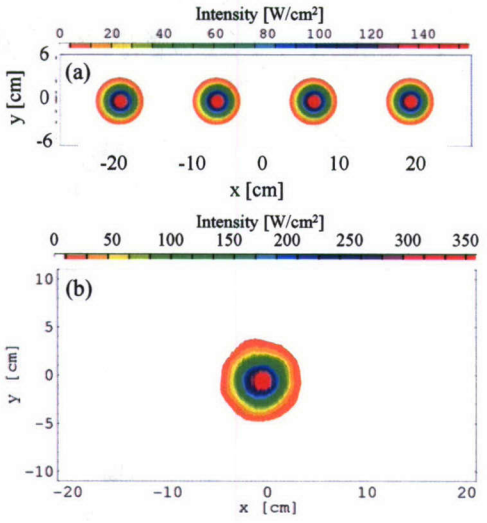

Figure 12: HELCAP simulation showing time-averaged transverse intensity profile of laser beams at (a) the source and (b) incoherently combined on target at a range of 1.2 km for turbulence strength $C_n^2 = 5\times10^{-14}\ \mathrm{m}^{-2/3}$, wind speed of 2.5 m/sec, aerosol scattering coefficient of 0.05 km^{-1}, and mechanical jitter of 2 μrad. The individual initial spot size is 2.5 cm and the combined spot size on target is ~ 5 cm.

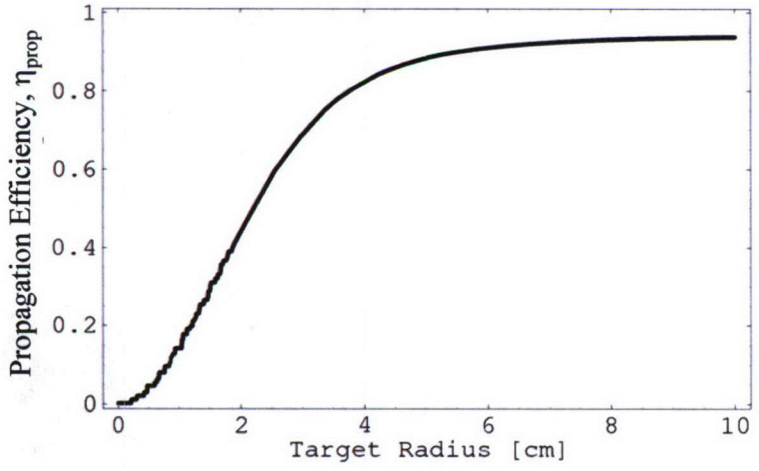

Figure 13: Propagation efficiency (ratio of power on target to transmitted power) versus target radius for the simulation of Fig. 12. Total transmitted power is 6.2 kW. Power within a 10 cm radius target at 1.2 km range is 5.8 kW, which corresponds to a propagation efficiency of 94%.